Electronic Supplementary Material (ESI) for Journal of Materials Chemistry A.

Supporting Information

Atomic-Level Characterization of Oxygen Storage Material $YBaCo_4O_{7+\delta}$ Synthesized at Low Temperature

Hsin-Hui Huang,[a*] Shunsuke Kobayashi,[a*] Toyokazu Tanabe,[b] Kaihei Komiyama,[c] Miwa Saito,[c] Teruki Motohashi [c] and Akihide Kuwabara [a]

[a]Nanostructures Research Laboratory, Japan Fine Ceramics Center, 2-4-1 Mutsuno, Atsuta-ku, Nagoya, 456-8587, Japan

[b]Department of Materials Science and Engineering, National Defense Academy, 1-10-20, Hashirimizu, Yokosuka, Kanagawa 239-0811, Japan

[c]Department of Materials and Life Chemistry, Faculty of Engineering, Kanagawa University, Kanagawa 221-8686, Japan

*Email: hsin-hui_huang@jfcc.or.jp, s_kobayashi@jfcc.or.jp

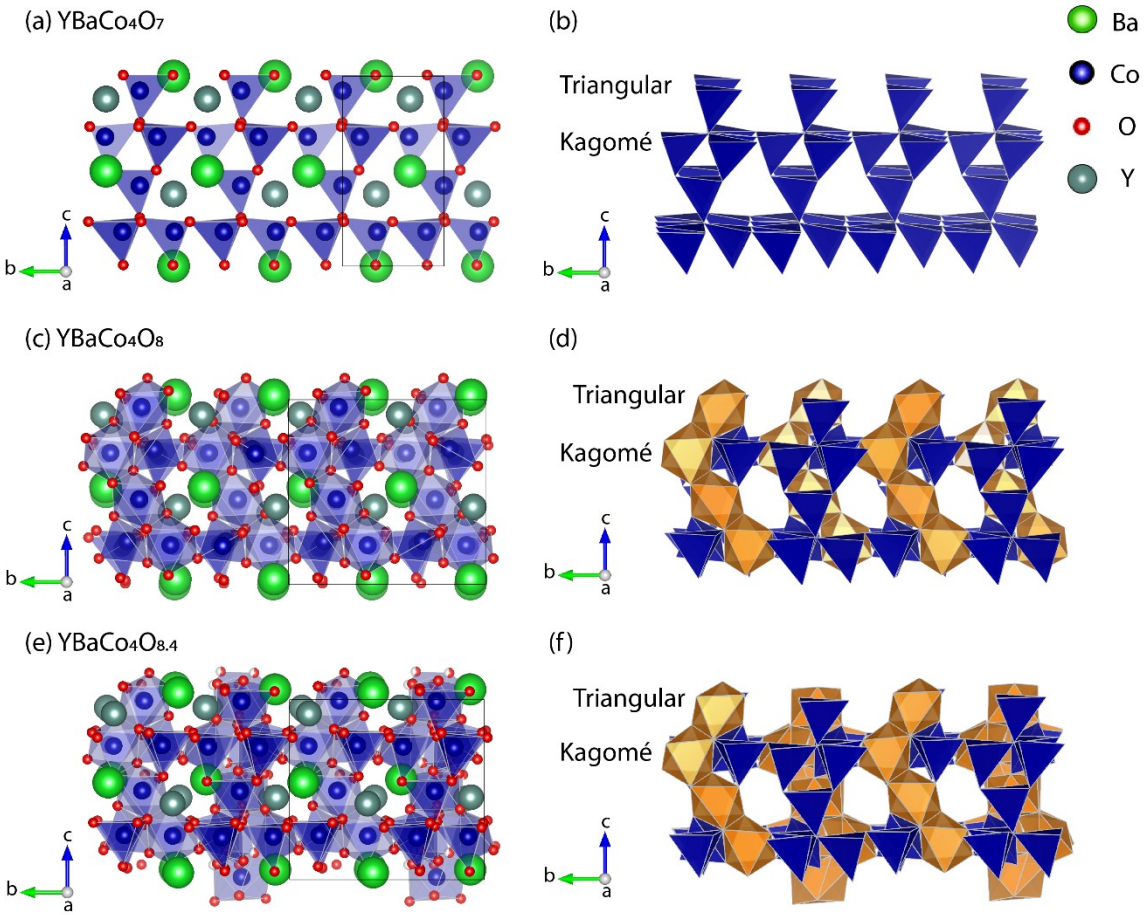

Figure S1. Schematic illustrations of the crystal structure of (a) $YBaCo_4O_7$ and (b) local geometry of the triangular and Kagomé layers. The crystal structure of (c)(d) oxygenated $YBaCo_4O_8$ and (e)(f) oxygenated $YBaCo_4O_{8.4}$. (d) and (f) show that the geometrical arrangement of CoO_4 tetrahedra partially converted into CoO_6 octahedra, as highlighted in orange. The difference between $YBaCo_4O_8$ and $YBaCo_4O_{8.4}$ is that more CoO_4 tetrahedra are converted into CoO_6 octahedra in the latter due to the larger amount of oxygen incorporated into the structure. The structural models of $YBaCo_4O_7$, $YBaCo_4O_8$, and $YBaCo_4O_{8.4}$ are adapted from references S1, S2, and S3, respectively. The illustrations were drawn by VESTA software.

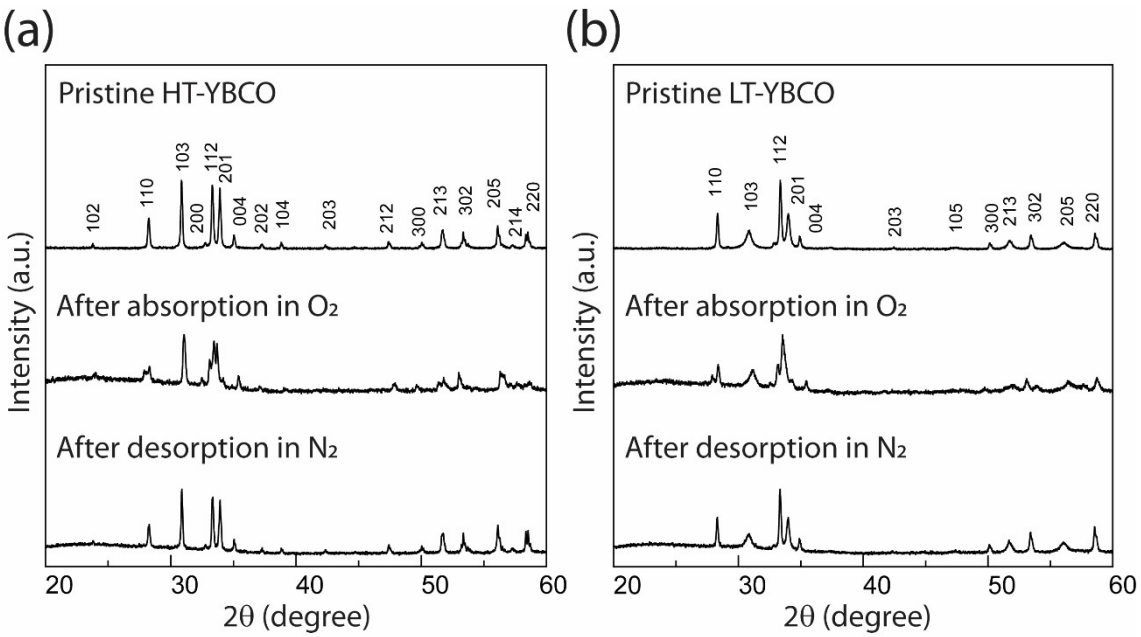

Figure S2. XRD patterns of (a) HT-YBCO and (b) LT-YBCO measured in the pristine state, after oxygen absorption, and oxygen desorption.

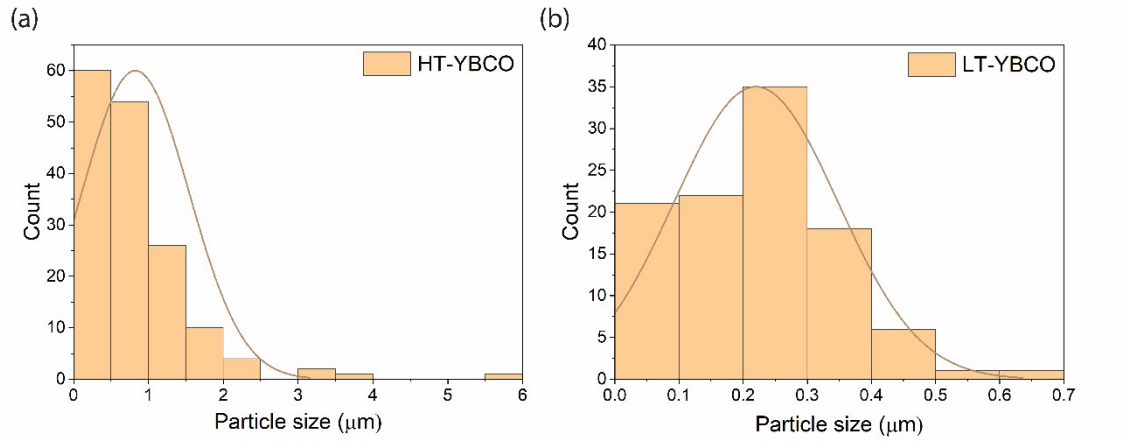

Figure S3. Histograms of the particle size distribution of pristine (a) HT-YBCO and (b) LT-YBCO.

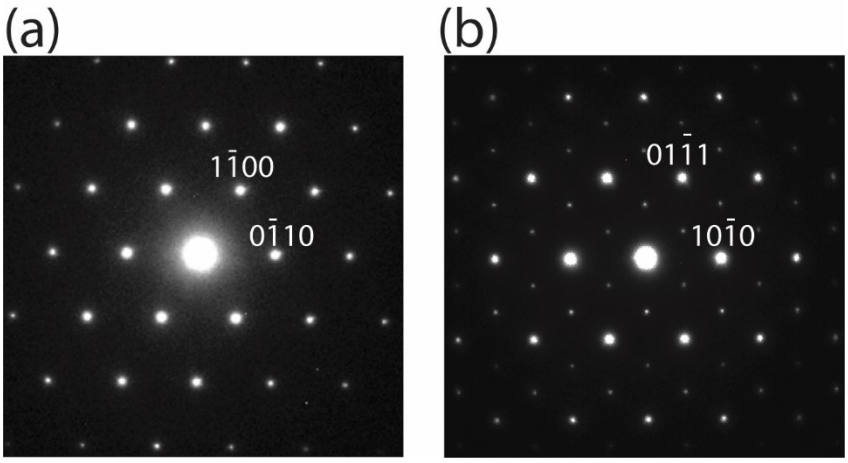

Figure S4. Electron diffraction patterns of pristine LT-YBCO viewed from the zone axes of (a) $[0001]$ and (b) $[1\bar{2}13]$ directions.

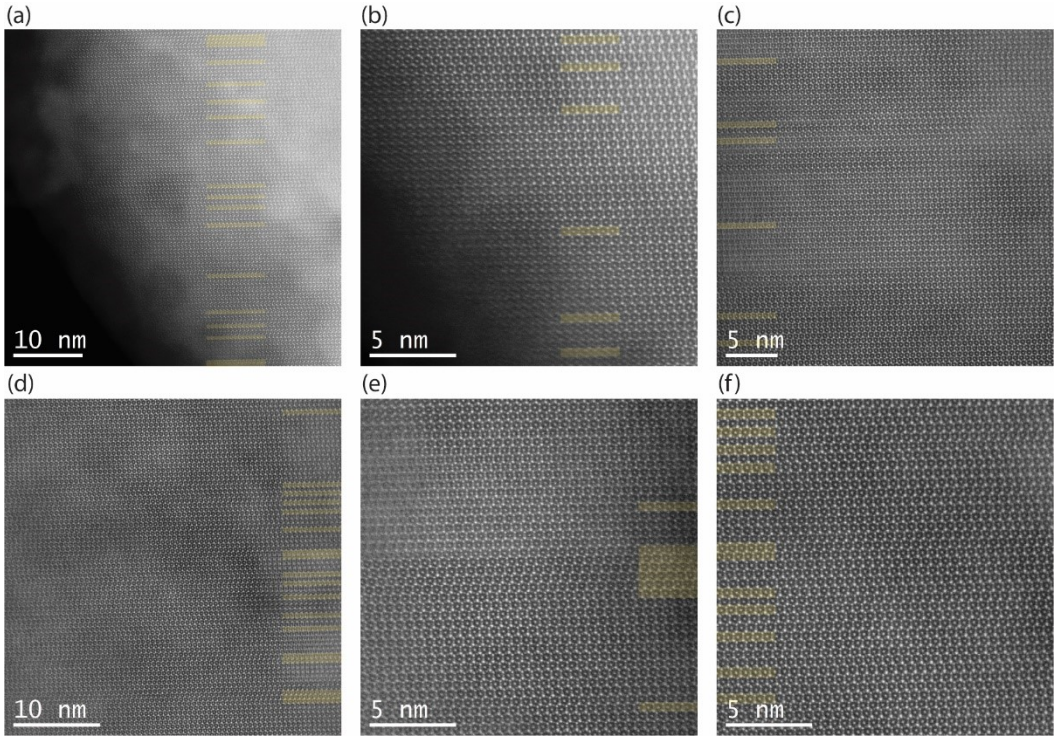

Figure S5. (a-f) HAADF-STEM images of pristine LT-YBCO taken in different regions. The stacking faults are highlighted in yellow.

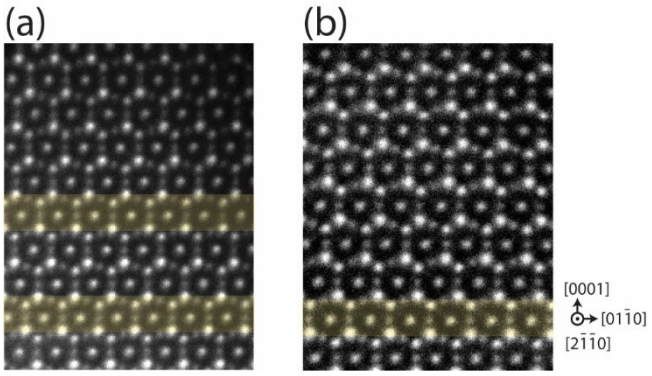

Figure S6. HAADF-STEM images of LT-YBCO after (a) oxygen absorption and (b) oxygen desorption. Stacking faults are indicated by yellow highlights.

Acquisition-time dependence

For the acquisition-time dependence, an area of approximately 100 × 100 nm^2 was selected on an annular dark-field image to obtain EELS data. Energy dispersion of 0.3 eV per channel was used to acquire the carbon K-edge. The total acquisition time was 42 s and the exposure time was 0.1 s per pixel.

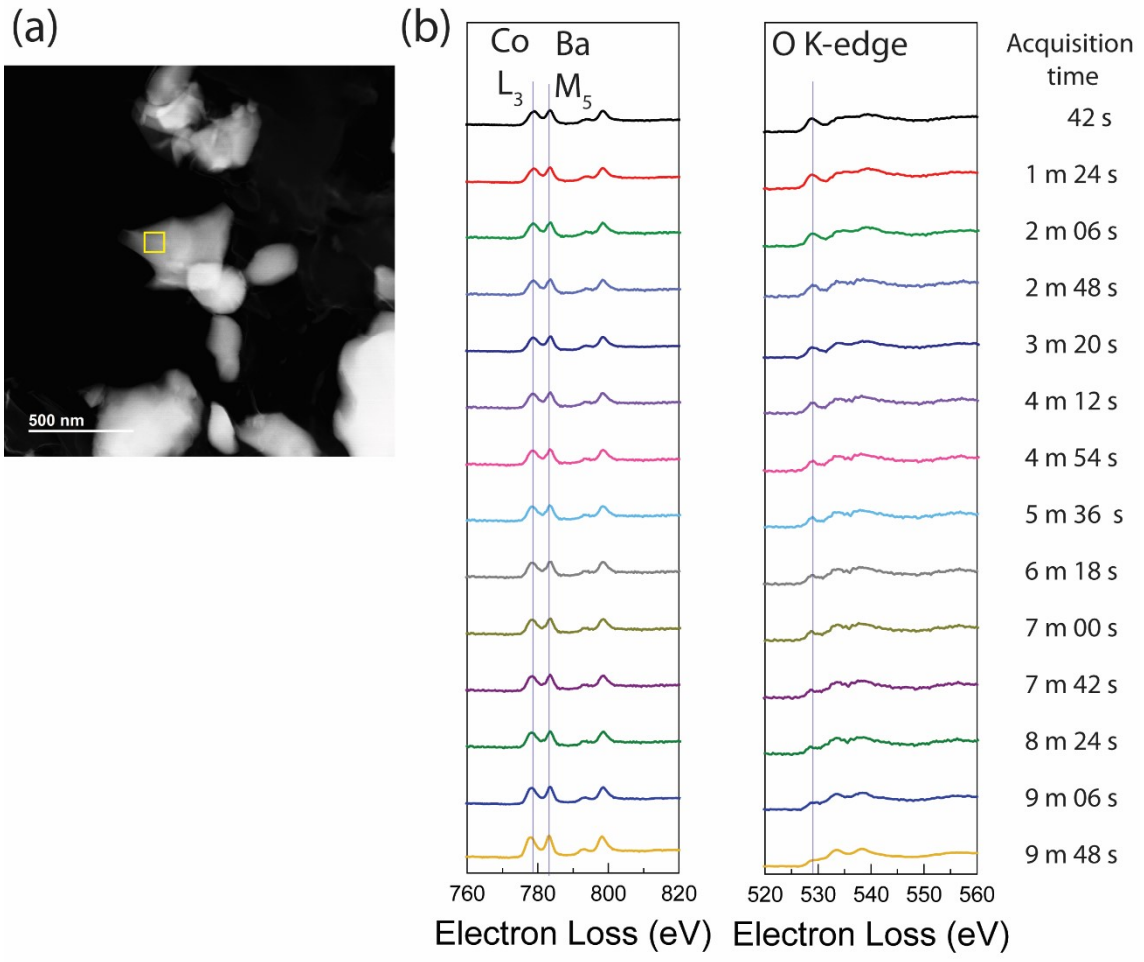

Figure S7. (a) HAADF-STEM image of the oxygenated LT-YBCO. (b) EEL spectra of the Co L, Ba M, and O K edges taken from the yellow rectangle area in (a) at acquisition time from short to long under the same condition. A peak shift of the Co L edge was found after an acquisition time of 5 min 36 s, indicating the reduction of cobalt upon oxygen release from the crystal lattice. Further exposure to electrons results in a diminishment of the onset (at 528.9 eV) in the O K edge, implying a full release of the absorbed oxygen.

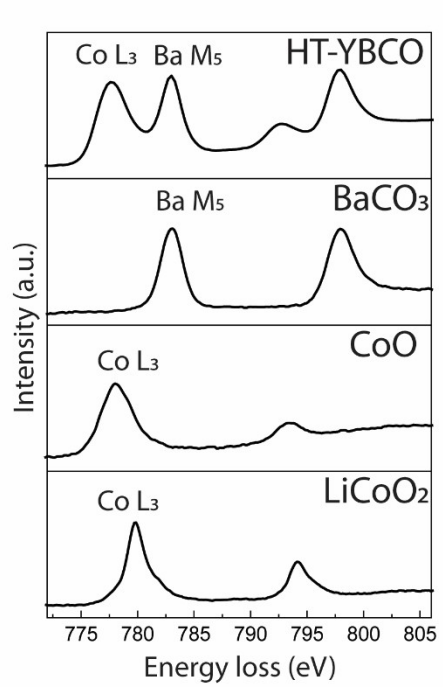

Figure S8. EEL spectra of the Co L and Ba M edges for the pristine HT-YBCO, $BaCO_3$, CoO, and $LiCoO_2$.

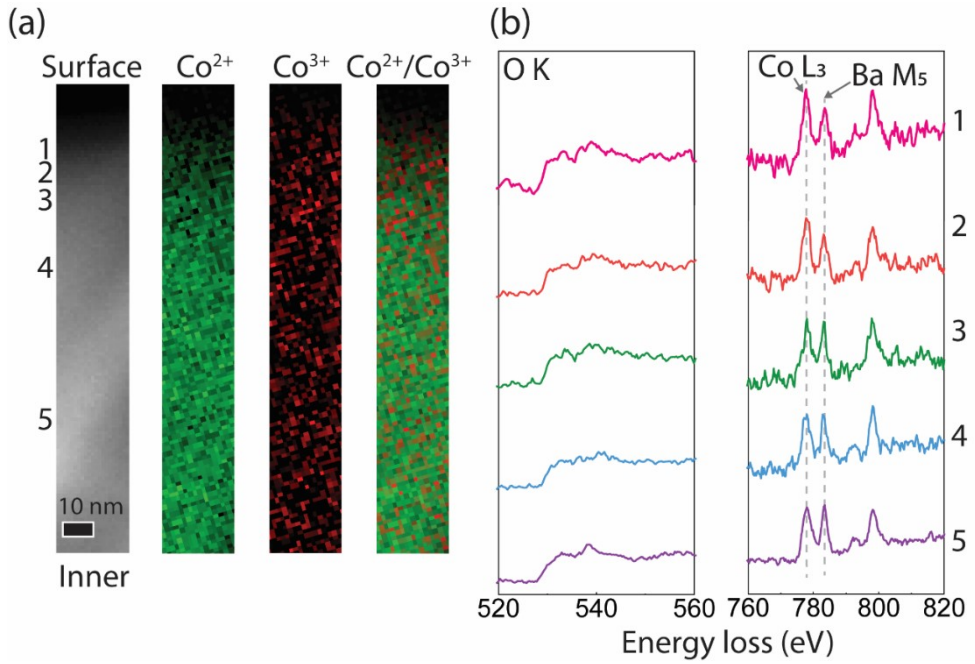

Figure S9. (a) ADF image of the pristine HT-YBCO particle near the surface and the corresponding MLLS fitting maps of Co^{2+}, Co^{3+}, and Co^{2+}/Co^{3+}, based on the references of CoO (Co^{2+}), $LiCoO_2$ (Co^{3+}) and $BaCO_3$ (Ba^{2+}). (b) EEL spectra of the O K, Co $L_{2,3}$ and Ba $M_{4,5}$ edges extracted from the horizontal lines 1 to 5 on the ADF image.

Surface state examinations of oxygenated HT-YBCO and LT-YBCO

The phase maps of Co^{2+}, Co^{3+}, and Co^{2+}/Co^{3+} overlap of oxygenated HT-YBCO and LT-YBCO were extracted and shown in Fig. S10a and S11a, respectively. The EEL spectra of Co $L_{2,3}$, Ba $M_{4,5}$, and O K edges obtained from the horizontal lines 1 (near the surface) to 5 (inner structure) labeled in ADF images are shown in Fig. S10b and S11b. It was found that oxygenated HT-YBCO and LT-YBCO show almost no shift in the peak position of Co L edge from the inner structure to near the surface of the particles. Furthermore, the measured peak position of Co L_3 edges of oxygenated HT-YBCO (778.8 eV) and oxygenated LT-YBCO (778.6 eV) are consistent with the values measured from the oxygenated YBCO at the inner structures (778.9 eV in HT-YBCO and 778.7 eV in LT-YBCO). It confirms that the entire particles of both oxygenated HT-YBCO and LT-YBCO are fully oxidized to their equilibrium states. In addition to that, it implies that the pathway of oxygen absorption is not disturbed by the surface effects in LT-YBCO.

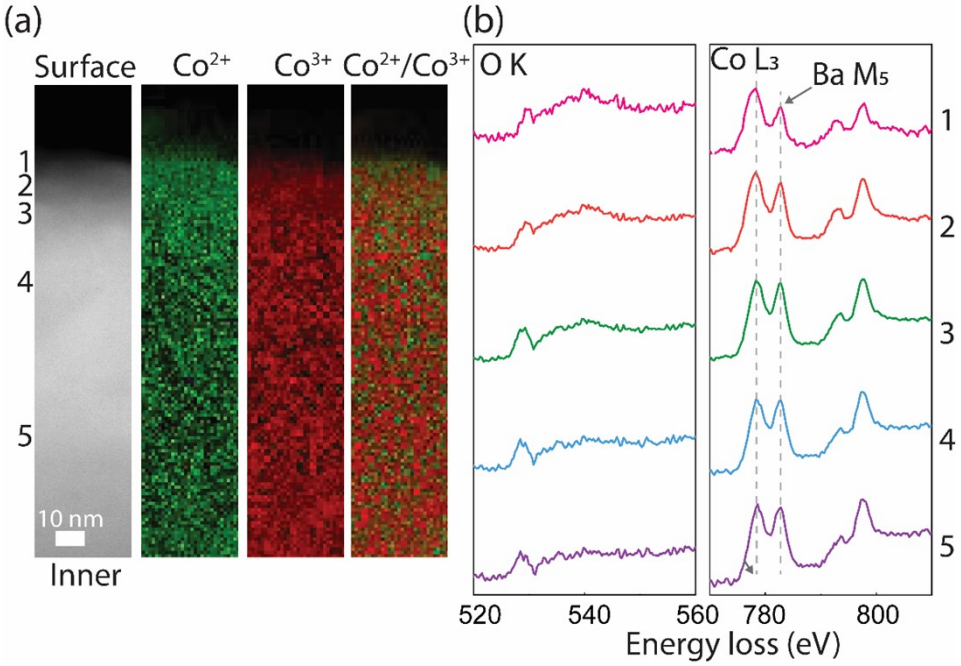

Figure S10. (a) ADF image of the oxygenated HT-YBCO particle near the surface and the corresponding Co^{2+}, Co^{3+}, and Co^{2+}/Co^{3+} maps using MLLS fitting approach with the reference spectra obtained from CoO (Co^{2+}), $LiCoO_2$ (Co^{3+}) and $BaCO_3$ (Ba^{2+}). (b) EEL spectra of the O K, Co $L_{2,3}$ and Ba $M_{4,5}$ edges extracted from the horizontal lines 1 to 5 on the ADF image.

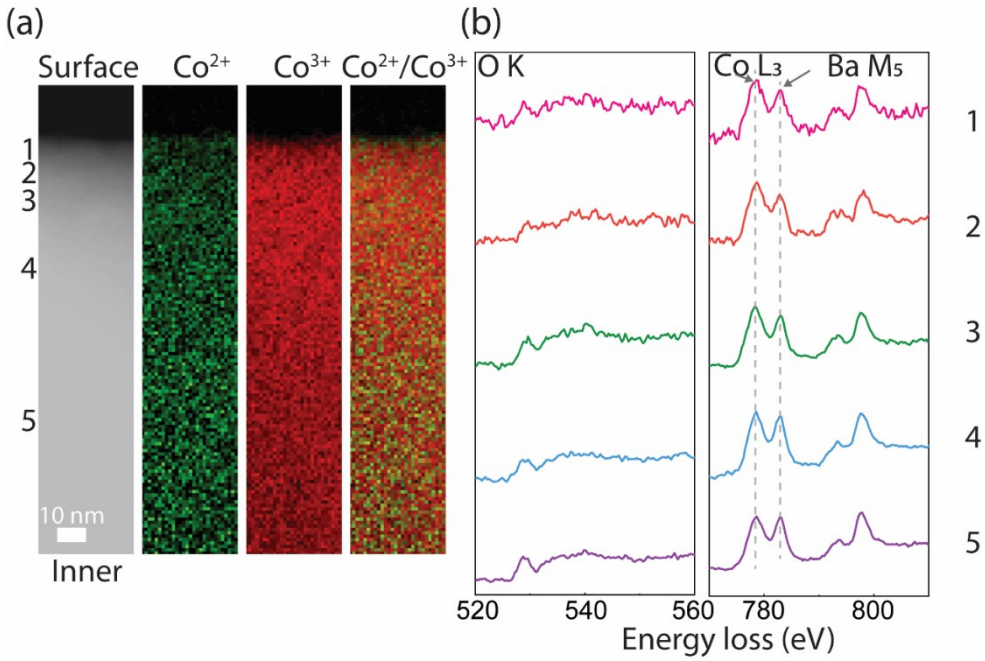

Figure S11. (a) ADF image of the oxygenated LT-YBCO particle near the surface and the corresponding MLLS fitting maps of Co^{2+}, Co^{3+}, and Co^{2+}/Co^{3+}, based on the references of CoO (Co^{2+}), $LiCoO_2$ (Co^{3+}) and $BaCO_3$ (Ba^{2+}). (b) EEL spectra of the O K, Co $L_{2,3}$, and Ba $M_{4,5}$ edges extracted from the horizontal lines 1 to 5 on the ADF image.

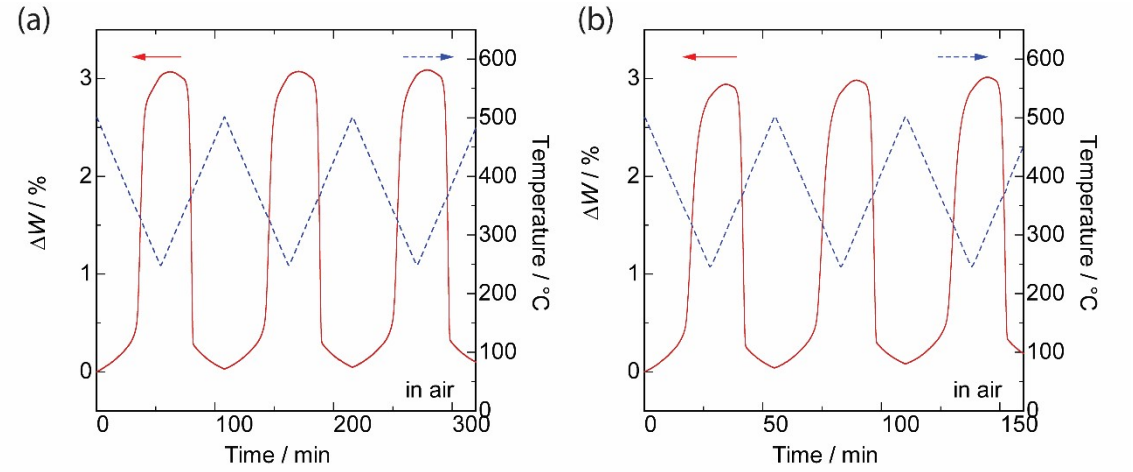

Figure S12. TG curves for HT-YBCO in flowing synthetic air upon temperature swing between 250 °C and 500 °C under heating/cooling rates of (a) 5 K/min and (b) 10 K/min. The sample temperature is also shown with a dotted curve.

References

S1. T. Komiyama, T. Motohashi, Y. Masubuchi, S. Kikkawa, Synthesis, *Materials Research Bulletin* 2010, **45**, 1527-1532.

S2. O. Chmaissem, H. Zheng, A. Huq, P.W. Stephens, J.F. Mitchell, *Journal of Solid State Chemistry* 2008, **181**, 664-672.

S3 N.V. Podberezskaya, N.B. Bolotina, V.Yu. Komarov, M.Yu. Kameneva, L.P. Kozeeva, A.N. Lavrov, A.I. Smolentsev, *Crystallography Reports* 2015, **60**, 484-492.